universe

MDPI

Article

On the Origin of Sodium Atoms in the Comae and Trails of Comets

Marco Fulle [1,*], Paolo Molaro [1,2] and Ilya Ilyin [3]

[1] INAF—Osservatorio Astronomico, Via Tiepolo 11, I-34143 Trieste, Italy; paolo.molaro@inaf.it
[2] IFPU—Institute for Fundamental Physics of the Universe, Via Beirut 2, I-34151 Trieste, Italy
[3] Leibniz Institute for Astrophysics Potsdam (AIP), An der Sternwarte 16, D-14482 Potsdam, Germany; ilyin@aip.de
* Correspondence: marco.fulle@inaf.it

Abstract

Background: The observed abundance ratios of alkali species in ground-based spectra of comets deviate from solar composition, suggesting alkali ejection from phenoxides reacting with carbon dioxide at the nucleus surface (alkali-phenoxide carbonylation). Methods: Here, we search for the alkali emissions in spectra of the coma and of the trail of Comet C/2023 A3 (Tsuchinshan-ATLAS) exploiting the double-fiber entrance of the high-resolution PEPSI spectrograph at the 8.4 m Large Binocular Telescope. Results: Spectra sampling the nucleus yield Na/K ratios 3.6 times higher than the chondritic value, and even higher ratios sampling the trail. This fact excludes photodesorption as the main sodium source, leaving sodium-phenoxide carbonylation at the surface of the main nucleus and the trail mininuclei as the primary sodium source. Conclusions: The nucleus temperature and the faint KI line exclude potassium-phenoxide carbonylation. For the first time, KI is detected in the trail of an Oort cloud comet, suggesting potassium photodesorbed from the trail mininuclei. Sodium-phenoxide carbonylation is at least six times more efficient than sodium photodesorption if the Na/K ratio in the C/2023 A3 nuclei is chondritic. Trails composed of sub-km-sized mininuclei may be common features of Oort cloud comets.

Keywords: Comets: general; Comets: C/2023 A3 Tsuchinshan-ATLAS; Oort cloud; molecular processes; techniques: spectroscopic

1. Introduction

This study examines the sources and abundances of the alkali elements sodium (Na), potassium (K) and lithium (Li) in comets. Sodium emission has been widely reported in cometary comae and tails [1–5], whereas potassium detections remain comparatively rare, having been identified to our knowledge only in comets C/1965 S1 [6], C/2011 L4 [7], C/2012 S1 [5], C/2020 F3 and C/2024 G3 [8]. In all cases, the Na/K atomic ratio significantly exceeds the chondritic value of $(Na/K)_c = 16$ [9]. The detection of the KI line in cometary spectra allowed Fulle et al. [8] to predict that a potassium tail should be observable in future comets.

To date, lithium has not been directly detected in cometary spectra. In contrast, laboratory mass spectrometry of the components of residues of dust particles from comet 81P/Wild 2 collected by the Stardust mission revealed Li, Na, and K abundances exceeding chondritic levels all within a factor of two [10]. The Li upper limit for comet C/2020 F3 is very stringent with $Na/Li > 3.4 \times 10^4$, a factor of >33 greater than the chondritic

Check for updates

Academic Editors: Emese Forgacs-Dajka, Csaba Kiss and Lorenzo Iorio

Received: 21 February 2026
Revised: 13 April 2026
Accepted: 15 May 2026
Published: 18 May 2026

Copyright: © 2026 by the authors. Licensee MDPI, Basel, Switzerland. This article is an open access article distributed under the terms and conditions of the Creative Commons Attribution (CC BY) license.

value of $(Na/Li)_c = 1036$ [9]. Li is synthesized during standard Big Bang nucleosynthesis and further enriched by novae to present values [11]. The value found in C/2020 F3 implies a Li abundance below the primordial value, a fact that leads to the formulation of a new mechanism for alkali ejection in comets due to alkali-phenoxide carbonylation, namely, the chemical reaction between alkali phenoxides and carbon dioxide inside the dust particles located at the nucleus surface followed by the protonation (e.g., by protons photodesorbed from dust hydrocarbons) of the produced alkali salicylates actually ejecting alkali atoms [8,12]. Laboratory data of the protonation of alkali phenoxides are not available. If this process was ejecting alkali atoms as efficiently as the protonation of salicylates at temperatures different than alkali-phenoxide carbonylation, then the strong production increase in sodium at $r \approx 0.8$ au and of potassium at $r \approx 0.5$ au [8] would remain unexplained.

Alkali-phenoxide carbonylation is activated when the cometary nucleus exceeds a limit temperature, which is 363 K for sodium and 473 K for potassium [12]. Available measurements of the surface temperature of the nucleus of Comet 67P/Churyumov-Gerasimenko (67P hereafter) by means of the Visible and Infrared Thermal Imaging Spectrometer (VIRTIS) instrument onboard the Rosetta mission showed that Hapi, the most active region during the inbound orbit, reached the gray-body temperatures, with the most probable value of 214 K at $r = 3.54$ au [13]. Here, we focus on spectra of Comet C/2023 A3 (Tsuchinshan-ATLAS), which is an Oort cloud comet first identified in Purple Mountain Observatory images and later independently recovered by the Asteroid Terrestrial impact Last Alert System (ATLAS) in February 2023. The spectra were taken at the heliocentric distances $0.81 \leq r \leq 0.83$ au (Table 1), where an active nucleus reaches gray-body temperatures $442 \leq T \leq 447$ K, consistent with sodium-phenoxide carbonylation and inconsistent with potassium-phenoxide carbonylation. The water-ice-enriched block (WEB) model [8,14] suggests lower equilibrium temperatures of 340 K at $r = 0.8$ au (in Table 5 of [8]) for a water-driven active nucleus. However, the Rosetta/VIRTIS data show that the surface dust particles where carbon dioxide may react with alkali phenoxides maintain higher non-equilibrium temperatures much closer to the gray-body ones.

Table 1. Log of observations, with one fiber located on the nucleus and another on the trail.

UT October 2024	Exposure s	Air Mass	r au	Δ au	$\dot{r}$ km/s	$\dot{\Delta}$ km/s	α deg	PA_r deg	PA_v deg	PA_o deg	ρ_o km	a_{Na} m/s^2	a_K m/s^2
26.09–26.11	3×720	1.9–2.4	0.812	0.774	+33.64	+58.02	77.6	71.6	239.8	225.1	5600	0.65	0.48
27.06–27.12	3×1800	1.6–2.9	0.831	0.808	+33.61	+58.80	74.6	71.4	238.3	225.2	5800	0.62	0.46

r and Δ: heliocentric and geocentric distances. α: phase angle. PA_r and PA_v: position angles of the antisolar and trailing orbit directions. PA_o and ρ_o: position angle and distance from the nucleus of the trail observation. a_{Na} and a_K: alkali antisunward acceleration due to solar radiation pressure (see Fulle et al. [7] for its computation).

2. Observations and Data Analysis

Comet C/2023 A3 was observed on 26 and 27 October 2024 with the Potsdam Echelle Polarimetric and Spectroscopic Instrument (PEPSI) at the Large Binocular Telescope (LBT, Mount Graham, Arizona) [15] in monocular mode (8.4 m), with a spectral coverage from 380 to 900 nm at a resolving power of $\lambda/\Delta\lambda$ = 130,000. A fiber was located on the nucleus and another at the distance ρ_o of 5600 and 5800 km and position angle PA_o of 239.8 and 238.3 deg, respectively (Table 1).

The comet was receding from Earth with radial velocities of 58.02 and 58.80 km s^{-1} at geocentric distances of 0.77 and 0.81 au in the nights of the 26 and 27 October 2024, respectively. The comet was also receding from the Sun with heliocentric radial velocities of 33.64 and 33.61 km s^{-1} at heliocentric distances of 0.81 and 0.83 au, respectively (Table 1). The heliocentric and geocentric radial velocities were calculated by using JPL's

(Jet Propulsion Laboratory, Pasadena, California) SPK solar system and C/2023 A3 BSP ephemeris files. On 26 October, the comet was observed from 2h05m UT to 2h37m UT in three couples (each per fiber) of different exposures at different Cross Dispersers (CDs), with sequence CD6 CD5 CD4 at an air mass increasing from 1.9 to 2.4; on 27 October, the comet was observed from 1h28m to 3h00m UT in three couples of different exposures, with sequence CD5 CD4 CD6 at an air mass increasing from 1.6 to 2.9: this observing procedure introduced different night-dependent atmospheric reddening at different spectrum orders.

The spectra were reduced as described in Strassmeier et al. [16] and calibrated by means of the spectra of the standard star HR7950, observed just after each sequence at an air mass of 1.4, fifty degrees east of the comet. The spectra were divided by the telluric synthetic Transmission of the AtmosPhere for AStronomical data (TAPAS) spectrum calculated for the time of observations and local atmospheric profile [17] and then offset to the solar-reflected rest frame. A Phoenix solar spectrum [18] was used to correct the comet ones, thus providing the calibrated average values of the dust continuum computed over the whole spectral range covered by CD4, CD5 and CD6, after the correction of the different reddening at different spectrum orders. This procedure increased the local continuum noise and introduced emission artifacts, due to the high air masses, so we measured the line intensities on flux-calibrated raw spectra. The dust continuum of the raw spectra was expected to be constant (as observed in comet C/2011 L4 [7]) because the spectral slope of the solar Planckian of −18%/100 nm at 600 nm was almost balanced by the spectral reddening of cometary dust of $+(12.5 \pm 1.5)$%/100 nm [19], with a systematic error <15% from the NaI to the KI wavelengths. Therefore, the raw spectra were flux-calibrated by normalizing them to the computed dust continuum, and offset to the rest frame of the comet, so that the standard air wavelength scale corresponded to atomic/molecular species (Figures 1–5). The dust continuum increased by 30% from 26 to 27 October (an increase higher than the slope error and than the noise of the nucleus-centered dust continuum), consistent with possible one-day changes in the total dust cross section both on the nucleus-centered coma and at the distance ρ_o, which is covered in less than one day if the dust velocity is $\geq$68 m s^{-1}.

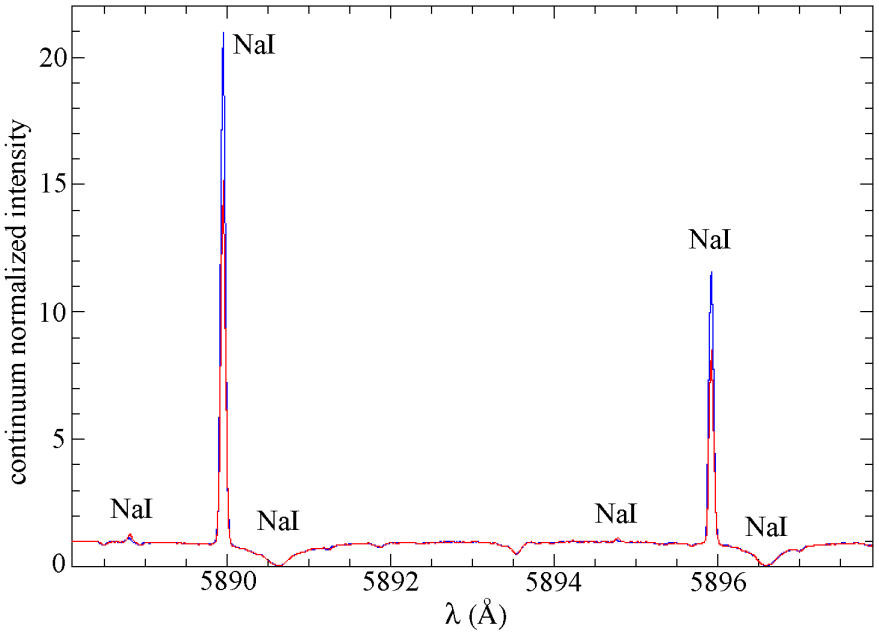


Figure 1. Nucleus spectra of comet C/2023 A3 in the NaI region taken on 26 (red line, continuum of 1.44×10^{-13} erg cm^{-2} s^{-1} Å^{-1}) and 27 October 2024 (blue line, continuum of 1.90×10^{-13} erg cm^{-2} s^{-1} Å^{-1}). The spectrum is corrected for by the geocentric velocity so that the telluric NaI emission line is blue-shifted by 58 km s^{-1} while the solar NaI absorption line is red-shifted by 34 km s^{-1}.

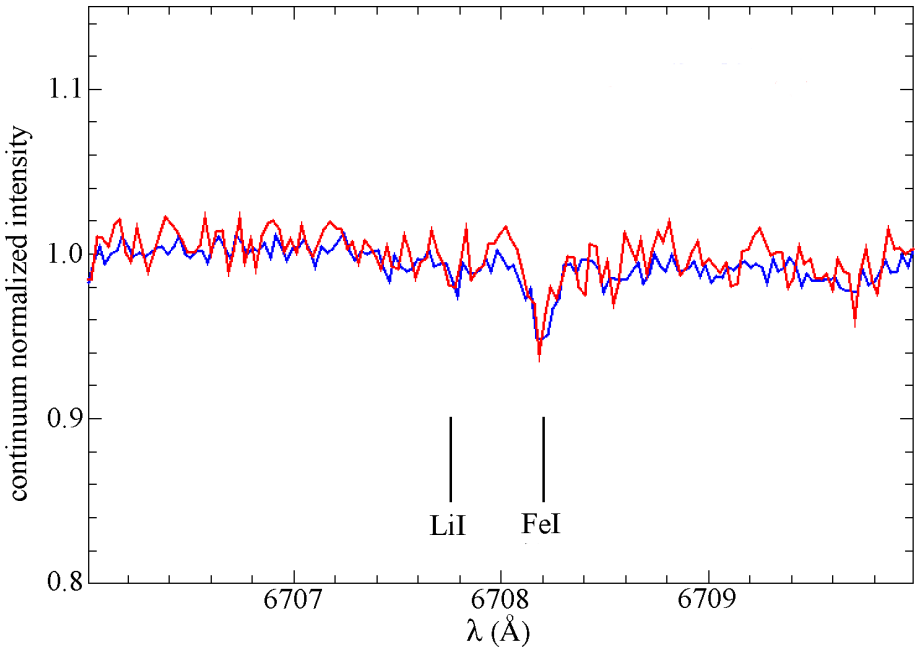


Figure 2. Nucleus spectra of comet C/2023 A3 in the LiI region taken on 26 (red line, continuum of 1.44×10^{-13} erg cm^{-2} s^{-1} Å^{-1}) and 27 October 2024 (blue line, continuum of 1.90×10^{-13} erg cm^{-2} s^{-1} Å^{-1}). The FeI solar absorption line at 6707.43 Å is red-shifted by 34 km s^{-1}.

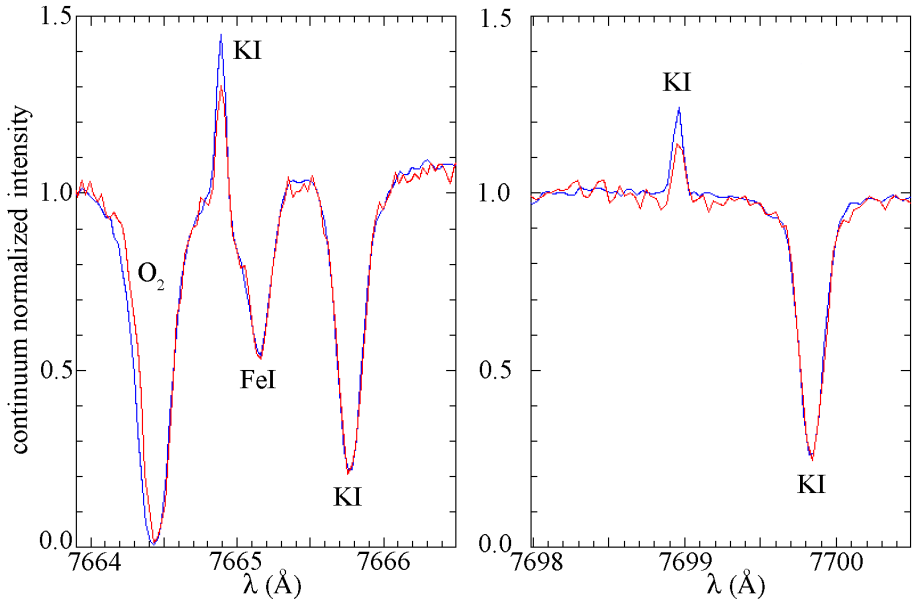


Figure 3. Nucleus spectra of comet C/2023 A3 in the KI region taken on 26 (red line, continuum of 1.44×10^{-13} erg cm^{-2} s^{-1} Å^{-1}) and 27 October 2024 (blue line, continuum of 1.90×10^{-13} erg cm^{-2} s^{-1} Å^{-1}). The solar KI absorption line is red-shifted by 34 km s^{-1}. The solar FeI absorption line at 7664.4 Å is red-shifted by 34 km s^{-1} and falls between the comet KI emission line and the solar KI absorption line. The strong absorption line at 7664.4 Å is an O_2 atmospheric line of the A band, which is slightly different between the two nights due to the different air mass.

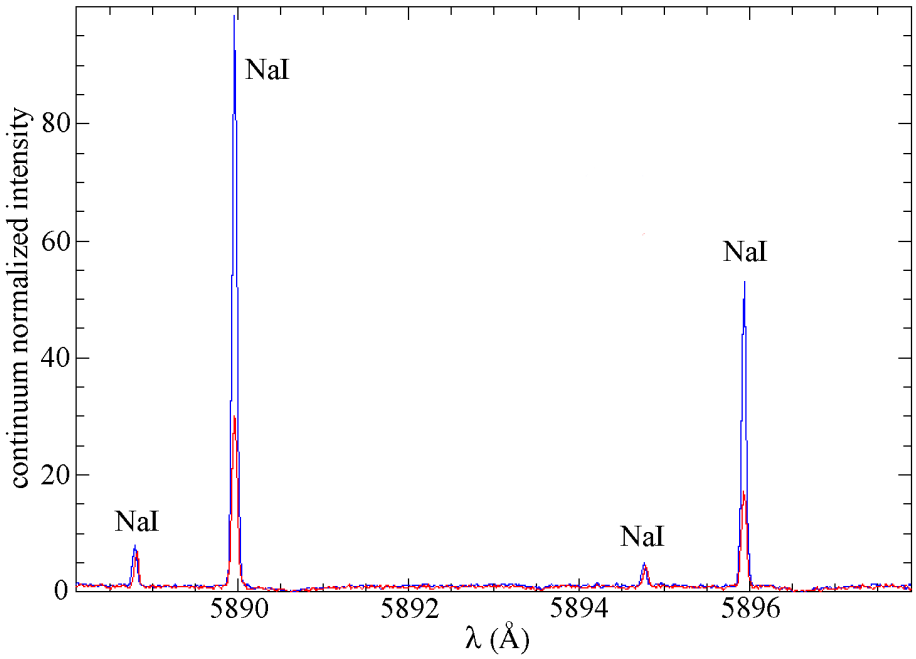


Figure 4. Trail spectra of comet C/2023 A3 in the NaI region taken on 26 (red line, continuum of 5.11×10^{-15} erg cm^{-2} s^{-1} Å^{-1}) and 27 October 2024 (blue line, continuum of 6.02×10^{-15} erg cm^{-2} s^{-1} Å^{-1}). The telluric Na emission line is blue-shifted by 58 km s^{-1}.

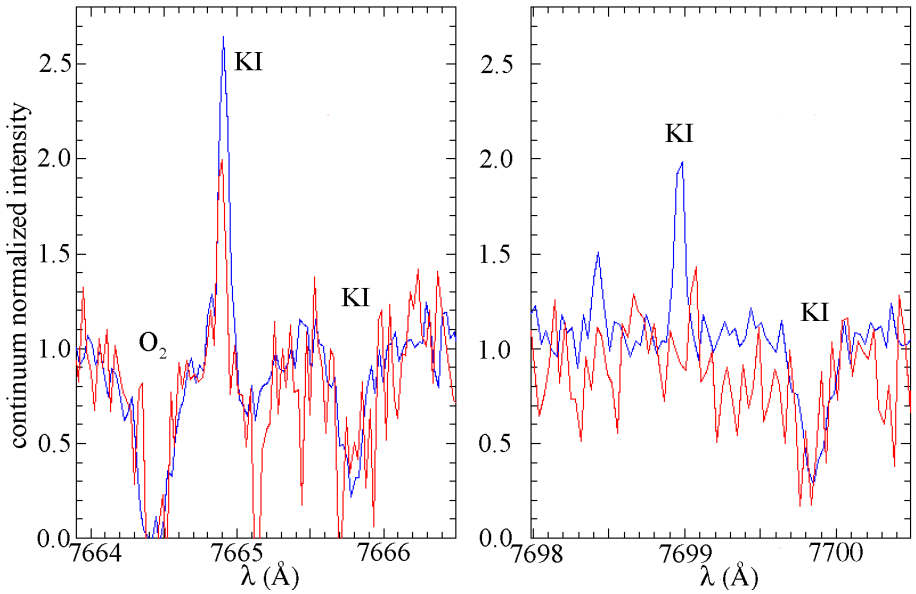


Figure 5. Trail spectra of comet C/2023 A3 in the KI region taken on 26 (red line, continuum of 5.11×10^{-15} erg cm^{-2} s^{-1} Å^{-1}) and 27 October 2024 (blue line, continuum of 6.02×10^{-15} erg cm^{-2} s^{-1} Å^{-1}). The solar KI absorption line is red-shifted by 34 km s^{-1}.

After the subtraction of the continuum, each emission line was fitted by a Gaussian, the FWHM of which varied from 60 to 80 mÅ, and converted to the intensities I (Table 2) by dividing each Gaussian area by 70 mÅ, thus facilitating the comparison with the lines in Figures 1–5. If the main sodium source is sodium-phenoxide carbonylation, then the I_{27N}/I_{26N} ratios provide the increase in the sunlit nucleus cross section due to its rotation, which is higher than the continuum increase during the same period because the wide dust velocity dispersion damps the brightness variations in the nucleus-centered dust coma. The abundances of sodium related to another atom x, Na/x (Table 2), are independent of

the absolute value of a flat continuum, depend on the g-factor g_x at 1 au computed by Fulle et al. [7] and are obtained from the line intensity I by means of the relationship

$$Na/x = (g_x/g_{Na})(I_{Na}/I_x). \quad (1)$$

Table 2. Line intensities and elemental abundances in C/2023 A3.

Atom	λ (Å)	I_{26N} (3σ)	I_{27N} (3σ)	I_{26T} (3σ)	I_{27T} (3σ)	$(\frac{Na}{x})_{26N}$	$(\frac{Na}{x})_{27N}$	$(\frac{Na}{x})_{26T}$	$(\frac{Na}{x})_{27T}$
Li	6707.78	<2.3	<1.9				>4500		
Na	5889.95	1315 ± 15	2415 ± 20	109.5 ± 1.5	379.3 ± 1.5	1	1	1	1
Na	5895.92	720 ± 15	1370 ± 20	59.1 ± 1.5	205.5 ± 1.5	1	1	1	1
K	7664.90	32.9 ± 2.1	59.7 ± 1.4	3.3 ± 1.6	7.0 ± 1.6	53 ± 12	53 ± 10	61 ± 37	77 ± 30
K	7698.96	15.0 ± 3.1	32.6 ± 1.4	<1.8	4.6 ± 1.8	70 ± 23	57 ± 10	>38	75 ± 35

Intensities I are in 10^{-15} erg cm^{-2} s^{-1} Å^{-1} units. I_{ij} specifies the intensities measured on the October day ($= i$) and on the nucleus ($j = N$) or on the trail ($j = T$). I_{Kij} specifies the average of the potassium intensities. $(Na/K)_N$ and $(Na/K)_T$ specify the averages of the nucleus and trail (Na/K) values, respectively. The two Na/K ratios refer to the couples of lines at $\lambda = 5889.95$ Å and $\lambda = 7664.90$ Å, and at $\lambda = 5895.92$ Å and $\lambda = 7698.96$ Å, respectively.

3. Discussion

The detection of faint KI lines in high-resolution spectra of C/2023 A3 implies that potassium is ejected by photodesorption only, thermal desorption being much less probable [4] and potassium-phenoxide carbonylation being impossible at $T \leq 447$ K. On the other hand, the detection of NaI lines implies two possible sources for sodium: photodesorption and sodium-phenoxide carbonylation. The fact that the Na/K ratio of cometary nuclei is likely chondritic [10,20] allows us to determine the efficiency of sodium-phenoxide carbonylation with respect to sodium photodesorption.

As in all previous comets with a measured Na/K ratio (Table 3), Na/K of C/2023 A3 exceeds the chondritic value (Table 2), with $(Na/K)_N = (3.6 \pm 0.9)(Na/K)_c$. The uncertainties affecting the Na/K ratios are higher than that of the continuum spectral slope. Munaretto et al. [21] analyzed the same spectra finding $(Na/K)_{27N} = 145 \pm 6$, which is 2–3 times higher than those shown in Table 2, with a similar uncorrected factor between the Na and K continuum, due to the color bias of a flux calibration not correcting the different atmospheric reddening of the comet and of the photometric standard star HR7950.

Table 3. Alkali abundances with respect to the chondritic ratios $(Na/K)_c$ and $(Na/Li)_c$ [6–8].

Comet	r au	$(Na/K)_N/(Na/K)_c$	$(Na/K)_T/(Na/K)_c$	$(Na/Li)_N/(Na/Li)_c$
C/1965 S1	0.14	3.1 ± 0.7		>32
C/2024 G3	0.15	1.6 ± 0.5		>1
C/2020 F3	0.36	1.9 ± 0.3		>33
C/2011 L4	0.46	3.4 ± 0.9		>7.7
C/2023 A3	0.83	3.6 ± 0.9	4.5 ± 2	>4.5

The sunward distance ρ_o excludes that the spectra outside the nucleus are polluted by alkali atoms ejected from the main nucleus towards the Sun, reaching the maximum sunward distance $\rho = v^2/(2a)$, where a is the antisunward acceleration due to the solar radiation pressure (Table 1) and $v = \sqrt{7.6085\, k\, T/m} = 1.25$ km s^{-1} at $T = 447$ K is the atom ejection velocity outside ten nucleus radii [22]; here, k is the Boltzmann constant and m is the molecular mass of water, because all alkali atoms are dragged at the velocity of the most abundant gas in the coma. We get $\rho \leq 1700$ km $\ll \rho_o$ for both sodium and potassium (Table 1), thus ruling out the alkali tail model [7] as a possible explanation of

$Na/K \gg (Na/K)_c$, because it predicts an increasing Na/K ratio from the assumed alkali source in the sunward coma to the nucleus, opposite to the actual data (Table 2).

All these facts exclude that sodium is ejected by thermal or photodesorption only, which, according to laboratory experiments [23], are expected to maintain a chondritic value both on the nucleus and on the coma dust, i.e., the same refractories mainly composing the nucleus itself. Mass fractionation at ejection is also inconsistent with the $(Na/Li)/(Na/Li)_c$ ratios higher than the $(Na/K)/(Na/K)_c$ ones (Table 3), opposite to what is expected according to the respective atomic masses. Significant sticking of alkali on coma dust would imply a strong increase in the Na/K ratio as r decreases [23], opposite to observations (Table 3). After ejection, the main fractionation is photoionization by the solar UV radiation [23], with lifetimes $\tau_{Na} = 1.3 \times 10^5$ s and $\tau_K = 3 \times 10^4$ s at $r = 0.83$ au [7], thus affecting the Na/K ratio by $\exp -\frac{\phi}{\tau_{Na} v} / \exp -\frac{\phi}{\tau_K v} = 1.018$, where $\phi = 870$ km is the fiber diameter at the comet. Therefore, the observed high Na/K ratios suggest that sodium is mainly produced by sodium-phenoxide carbonylation, thus more efficient than photodesorption. In this case, the alkali source should have a volume big enough to produce carbon dioxide, corresponding to sizes of some tens of meters [8], i.e., mininuclei populating a trail. A sodium trail was actually observed in C/2024 G3 [8]. Its dynamical analysis constrained its origin in the Oort cloud, where the galactic tides injecting C/2024 G3 towards the Sun possibly fragmented it into bodies larger than 30 m [8]. A sodium trail is also consistent with the very asymmetric C/2006 P1 NaI line along the comet-orbit-oriented spectrograph slit [4,8] and with the location of the fiber outside the nucleus of C/2023 A3 (Table 1). Here, we check if such a scenario is consistent with all the available data.

The very faint KI lines (a factor of >300 fainter than all other previous KI detections, which occurred at $r < 0.5$ au) suggest potassium photodesorption. In all previous KI observations, potassium-phenoxide carbonylation was the main source of potassium atoms, because photodesorption could have been more efficient than in C/2023 A3 by a factor of ≈3 (given by the squared ratio of the observation heliocentric distances) times the ratio of the respective nucleus cross sections, which is ≪100. The KI lines are as intense as the continuum on the trail (Figure 5), but much less intense than the continuum on the nucleus (Figure 3), where some contribution from the nucleus added to that from the dust would imply the opposite if potassium were photodesorbed from dust. A reliable continuum-independent source of potassium is photodesorption from the trail mininuclei, the volume of which can be estimated because photodesorption depends on the sunlit cross section of the source. We computed that the trail mininuclei had a total sunlit cross section $I_{K26T}/I_{K26N} = (23 \pm 18)\%$ of the main nucleus on 26 October, and $I_{K27T}/I_{K27N} = (16 \pm 12)\%$ on 27 October, both consistent with the storage of CO_2 ice inside them and with the expected size of trail mininuclei [8] at the distance ρ_o from the main nucleus (Table 1).

The fact that the KI line intensities are inconsistent with dust as the source of potassium further supports sodium-phenoxide carbonylation as the main sodium source. Sodium-phenoxide carbonylation depends on the nucleus surface area with $T > 363$ K, rather than on the sunlit nucleus cross section. Let us assume that sodium-phenoxide carbonylation is a factor of $f = 10$ more efficient than photodesorption in ejecting sodium atoms. In order to explain the highest Na/K ratio in Table 2, namely, $(Na/K)_{27Tmax} = 110$, it is sufficient that $(Na/K)_{27Tmax}/[(Na/K)_c(f+1)] \approx 70\%$ of the average trail mininuclei's surface had $T > 363$ K. If the whole mininuclei's surface had $T > 363$ K, then $(Na/K)_T = (Na/K)_c(f+1)$, namely, $(Na/K)_c f$ from sodium-phenoxide carbonylation and $(Na/K)_c$ from photodesorption. It follows that the lower limit of the efficiency ratio between sodium-phenoxide carbonylation and photodesorption is $f_{min} = (Na/K)_{27Tmax}/(Na/K)_c - 1 \approx 6$, which provides the highest possible area frac-

tion of trail mininuclei at $T > 363$ K: $(Na/K)_{26T}/[(Na/K)_c(f_{min}+1)] = (56 \pm 34)\%$ on 26 October and $(Na/K)_{27T}/[(Na/K)_c(f_{min}+1)] = (68 \pm 32)\%$ on 27 October. For the main nucleus, the highest possible area fraction at $T > 363$ K is $(Na/K)_N/[(Na/K)_c(f_{min}+1)] = (61 \pm 24)\%$, consistent with the expected source of carbon dioxide, i.e., the water-poor nucleus matrix covering about 90% of 67P's nucleus surface [13,14]. The trail mininuclei may have very different shape and temperature distribution, i.e., more variable Na/K ratios.

From 8 to 11 October 2024, the Solar and Heliospheric Observatory (SOHO) spacecraft observed C/2023 A3 at an angle of 3–8 deg between the comet orbital plane and the line of sight (versus 63 deg of C/2024 G3 in mid January 2025), preventing the detection of any sodium trail because projected on a much brighter dust tail (Figure 6). Sodium emission may be the only way to detect trails of Oort cloud comets. Alkali-phenoxide carbonylation requires production of carbon dioxide, which occurs in the water-poor matrix of nuclei, according to the WEB model [8,14]. At $r < 4$ au, such a matrix does not eject dust, consistent with the SOHO observations of the C/2024 G3 trail [8]. These SOHO observations are inconsistent with usual water-driven dust ejection: the dust continuum of, e.g., C/2023 A3 overcomes the sodium brightness at bandwidths larger than 1 nm (Figure 4), so that the dust trail should be visible at all wavelengths. It follows that the brightness slope of the dust coma of C/2023 A3 and C/2024 G3 is not affected by the presence of trail mininuclei. Degassing without any dust ejection has been inferred from non-gravitational perturbations of the orbits of 1I/'Oumuamua and of other dark comets [24,25]. Also, a direct detection of trail mininuclei of Oort cloud comets is challenging. Their distance from the main nucleus is inversely proportional to their size [8], so that the trail mininuclei's brightness is inversely proportional to the squared distance from the main nucleus, i.e., much steeper than the brightness slope of a steady dust coma. Since the main nucleus is hidden by the much brighter inner dust coma, this occurs even more for the trail mininuclei. The biggest mininuclei, closest to the main nucleus, might be affected by significant rocket effects due to anisotropic ejection of carbon dioxide spreading them in a cloud surrounding the main nucleus, i.e., a possible additional risk for the ESA Comet Interceptor Mission [26].

As in all previous spectra of comets, lithium was not detected, because the expected ratio was $Na/Li > (Na/Li)_c f_{min} = 6 \times 10^3$ in case of lithium photodesorption, and $Na/Li > 10^7$ in case of lithium-phenoxide carbonylation [8], both higher than the measured lower limit (Table 2), which was improved by averaging the values measured on 26 and 27 October. The lower limits measured on the trail were lower than $(Na/Li)_c$. The measured lower limit $Na/Li > 3.4 \times 10^4$ of comet C/2020 F3 Neowise [8] is still consistent with lithium photodesorption if $f_{min} > 33$ during those observations. In Table 3, the values of C/1965 S1 may be affected by the saturation of the NaI lines in the photographic spectra, thus of very uncertain intensity because extrapolated. The decrease in Na/K of the other comets towards chondritic values as r decreases is consistent with an increasing efficiency of potassium-phenoxide carbonylation as the nucleus temperature increases. The release of potassium should also build up an atomic tail, providing information on the distribution of this cometary component.

https://doi.org/10.3390/universe12050146

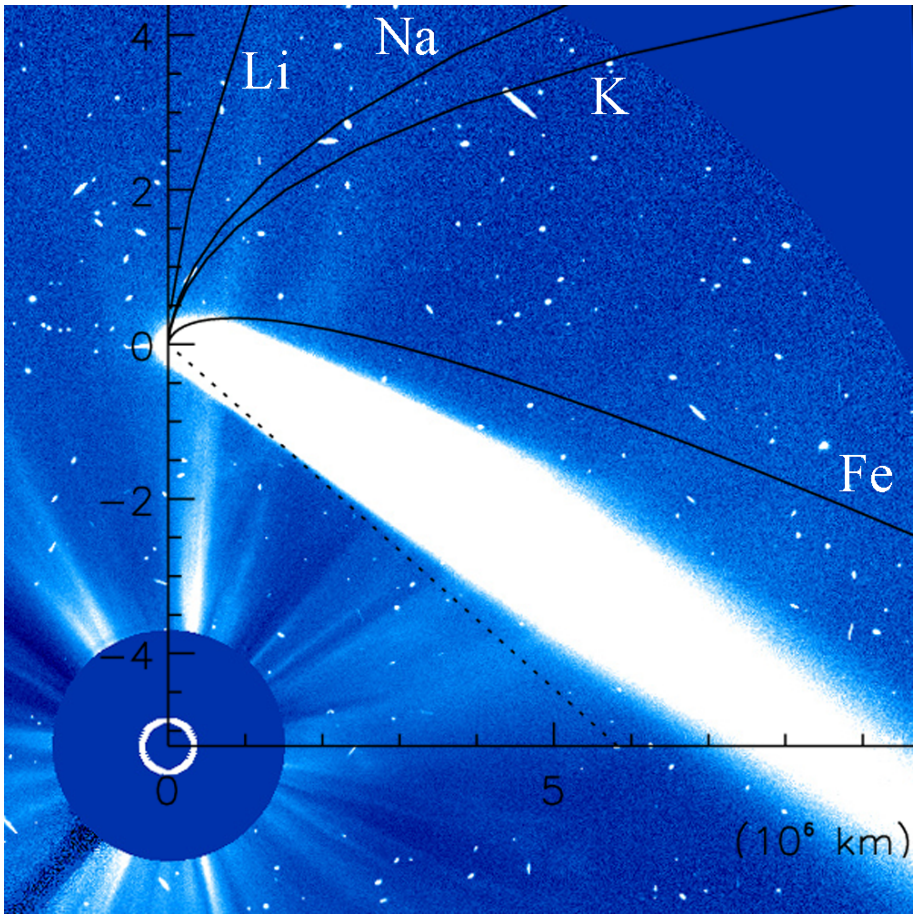


Figure 6. Comet C/2023 A3 observed on 2024 October 9.87 UT at $r = 0.509$ au by the SOHO spacecraft in the clear passband from 400 to 850 nm. Continuous curved lines: predicted atomic neutral tails [8], too faint to be visible. The nucleus and dust were too cold to release iron atoms. Dotted line: Comet orbit fitting the predicted sodium trail, which is hidden by the dust tail if shorter than 2×10^6 km.

4. Conclusions

1. We detected NaI and KI emission lines in very high resolution LBT/PEPSI spectra measured on the nucleus and on the trail of C/2023 A3 (Tsuchinshan-ATLAS).
2. The C/2023 A3 nucleus was too cold to allow potassium-phenoxide carbonylation but warm enough to allow sodium-phenoxide carbonylation.
3. The KI line was a factor of >300 fainter than all previous detections, consistent with potassium ejection by photodesorption.
4. We suggested trail mininuclei as the most probable source of alkali observed outside the nucleus. In this case, the ratios of potassium KI lines intensities allowed us to estimate the sizes of the trail mininuclei ejecting alkali atoms. These sizes were consistent with the production of carbon dioxide reacting with sodium phenoxides.
5. The Na/K ratios measured on the nucleus were a factor of 3.6 higher than the chondritic value, and even higher on the trail, thus excluding photodesorption and thermal desorption as the main sodium source.
6. A chondritic Na/K ratio in the nuclei of C/2023 A3 is consistent with all the performed measurements if the sodium-phenoxide carbonylation is at least a factor of six more efficient than sodium photodesorption in ejecting neutral sodium atoms.
7. As predicted by the alkali-phenoxide carbonylation model, lithium emission LiI was not detected in the spectra of C/2023 A3.
8. A trail of mininuclei big enough to allow alkali-phenoxide carbonylation may be a common feature of Oort cloud comets.

Author Contributions: Conceptualization, M.F. and P.M.; methodology, M.F.; software, I.I.; validation, M.F., P.M. and I.I.; writing—original draft preparation, M.F.; writing—review and editing, P.M. and I.I. All authors have read and agreed to the published version of the manuscript.

Funding: This research received no external funding.

Data Availability Statement: Data are available at the Large Binocular Telescope Archive https://archive.lbto.org (accessed on 23 November 2025).

Acknowledgments: We thank two anonymous reviewers and Marco Micheli for constructive discussions which significantly improved the paper.

Conflicts of Interest: The authors declare no conflicts of interest.

References

1. Combi, M.R.; Di Santi, M.A.; Fink, U. The Spatial Distribution of Gaseous Atomic Sodium in the Comae of Comets: Evidence for Direct Nucleus and Extended Plasma Sources. *Icarus* **1997**, *130*, 336–354. [CrossRef]
2. Rauer, H.; Arpigny, C.; Manfroid, J.; Cremonese, G.; Lemme, C. The spatial sodium distribution in the coma of comet Hale-Bopp (C/1995 O1). *Astron. Astrophys.* **1998**, *334*, L61–L64.
3. Watanabe, J.-I.; Kawakita, H.; Furusho, R.; Fujii, M. Heliocentric Dependence of the Sodium Emission of Comet 153P/Ikeya-Zhang. *Astrophys. J.* **2003**, *585*, L159–L162. [CrossRef]
4. Leblanc, F.; Fulle, M.; López Ariste, A.; Cremonese, G.; Doressoundiram, A; Sainz Dalda, A.; Gelly, B. Comet McNaught C/2006 P1: Observation of the sodium emission by the solar telescope THEMIS. *Astron. Astrophys.* **2008**, *482*, 293–298. [CrossRef]
5. McKay, A.; Cochran, A.; Dello Russo, N.; Weaver, H.; Vervack, R.; Harris, W.; Kawakita, H.; DiSanti, M.; Chanover, N.; Tsvetanov, Z. Evolution of fragment-species production in comet C/2012 S1 (ISON) from 1.6 au to 0.4 au. In Proceedings of the Asteroids, Comets, Meteors 2014 Conference, Helsinki, Finland, 30 June–4 July 2014.
6. Preston, G.W. The spectrum of Ikeya-Seki (1965f). *Astrophys. J.* **1967**, *147*, 718–742. [CrossRef]
7. Fulle, M.; Molaro, P.; Buzzi, L.; Valisa, P. Potassium Detection and Lithium Depletion in Comets C/2011 L4 (Panstarrs) and C/1965 S1 (Ikeya-Seki). *Astrophys. J. Lett.* **2013**, *771*, L21. [CrossRef]
8. Fulle, M.; Molaro, P.; Rotundi, A.; Tonietti, L.; Aletti, A.; Buzzi, L.; Valisa, P. Alkali phenoxides in comets. *Astron. Astrophys.* **2025**, *699*, A110. [CrossRef]
9. Lodders, K. Solar System Abundances and Condensation Temperatures of the Elements. *Astrophys. J.* **2003**, *591*, 1220–1247. [CrossRef]
10. Flynn, G.J.; Bleuet, P.; Borg, J.; Bradley, J.P.; Brenker, F.E.; Brennan, S.; Bridges, J.; Brownlee, D.E.; Bullock, E.S.; Burghammer, M.; et al. Elemental Compositions of Comet 81P/Wild 2 Samples Collected by Stardust. *Science* **2006**, *314*, 1731–1735. [CrossRef]
11. Molaro, P. The problem of Lithium and the other Light Elements Deuterium, Beryllium and Boron. *Mem. SAIt* **2023**, *94*, 22–27.
12. Kojčinović, A.; Likozar, B.; Grilc, M. Mechanism, Kinetics and Modelling of Phenol Carboxylation Reactions with CO_2. *Int. J. Mol. Sci.* **2024**, *25*, 12923. [CrossRef]
13. Ciarniello, M.; Fulle, M.; Tosi, F.; Mottola, S.; Capaccioni, F.; Bockelée-Morvan, D.; Longobardo, A.; Raponi, A.; Filacchione, G.; Rinaldi, G.; et al. Comparison of a pebbles-based model with the observed evolution of the water and carbon dioxide outgassing of comet 67P/Churyumov-Gerasimenko. *Mon. Not. R. Astron. Soc.* **2023**, *523*, 5841–5852. [CrossRef]
14. Ciarniello, M.; Fulle, M.; Raponi, A.; Filacchione, G.; Capaccioni, F.; Rotundi, A.; Rinaldi, G.; Formisano, M.; Magni, G.; Tosi, F.; et al. Macro and micro structures of pebble-made cometary nuclei reconciled by seasonal evolution. *Nat. Astron.* **2022**, *6*, 546–553. [CrossRef]
15. Strassmeier, K.G.; Ilyin, I.; Järvinen, A.; Weber, M.; Woche, M.; Barnes, S.I.; Bauer, S.-M.; Beckert, E.; Bittner, W.; Bredthauer, R.; et al. PEPSI: The high-resolution échelle spectrograph and polarimeter for the Large Binocular Telescope. *Astron. Nach.* **2015**, *336*, 324–361. [CrossRef]
16. Strassmeier, K.G.; Ilyin, I.; Steffen, M. PEPSI deep spectra. I. The Sun-as-a-star. *Astron. Astrophys.* **2018**, *612*, A44. [CrossRef]
17. Lallement, R.; Bertaux, J.L.; Ferron, S.; Boonne, C.; Richard, E.; Lefèvre, F.; Smoker, J.V. Transmission of the AtmosPhere for AStronomical data: TAPAS upgrade. *Astron. Astrophys.* **2025**, *701*, A200. [CrossRef]
18. Hauschildt, P.H.; Barman, T.; Baron, E.; Aufdenberg, J.P.; Schweitzer, A. The NewEra model grid. *Astron. Astrophys.* **2025**, *698*, A47. [CrossRef]
19. Bertini, I.; La Forgia, F.; Tubiana, C.; Güttler, C.; Fulle, M.; Moreno, F.; Frattin, E.; Kovacs, G.; Pajola, M.; Sierks, H.; et al. The scattering phase function of comet 67P/Churyumov-Gerasimenko coma as seen from the Rosetta/OSIRIS instrument. *Mon. Not. R. Astron. Soc.* **2017**, *469*, S404–S415. [CrossRef]
20. Wurz, P.; Rubin, M.; Altwegg, K.; Balsiger, H.; Berthelier, J.-J.; Bieler, A.; Calmonte, U.; De Keyser, J.; Fiethe, B.; Fuselier, S.A.; et al. Solar wind sputtering of dust on the surface of 67P/Churyumov-Gerasimenko. *Astron. Astrophys.* **2015**, *583*, A22. [CrossRef]

21. Munaretto, G.; Cremonese, G.; Cambianica, P.; Brunetto, R.; Aléon, J.; Aléon-Toppani, A.; Mura, A.; Ilyin, I.; Cusano, F.; Kuhn, O.; et al. High Resolution Spectroscopy of Comet C/2023 A3 (Tsuchinshan-ATLAS): Insight into Sodium, Potassium and Lithium abundances. In Proceedings of the EPSC-DPS Joint Meeting 2025 (EPSC-DPS2025), Helsinki, Finland, 7–12 September 2025; p. 1369.
22. Zakharov, V.V.; Rodionov, A.V.; Fulle, M.; Ivanovski, S.L.; Bykov, N.Y.; Della Corte, V.; Rotundi, A. Practical relations for assessments of the gas coma parameters. *Icarus* **2021**, *354*, 114091. [CrossRef]
23. Leblanc, F.; Doressoundiram, A. Mercury exosphere. II. The sodium/potassium ratio. *Icarus* **2011**, *211*, 10–20. [CrossRef]
24. Micheli, M.; Farnocchia, D.; Meech, K.J.; Buie, M.W.; Hainaut, O.R.; Prialnik, D.; Schörghofer, N.; Weaver, H.A.; Chodas, P.W.; Kleyna, J.T.; et al. Non-gravitational acceleration in the trajectory of 1I/2017 U1 ('Oumuamua). *Nature* **2018**, *559*, 223–226. [CrossRef]
25. Seligman, D.Z.; Farnocchia, D.; Micheli, M.; Hainaut, O.R.; Hsieh, H.H.; Feinstein, A.D.; Chesley, S.R.; Taylor, A.G.; Masiero, J.; Meech, K.J. Two distinct populations of dark comets delineated by orbits and sizes. *Proc. Natl. Acad. Sci. USA* **2024**, *121*, e2406424121. [CrossRef]
26. Jones, G.H.; Snodgrass, C.; Tubiana, C.; Küppers, M.; Kawakita, H.; Lara, L.M.; Agarwal, J.; André, N.; Attree, N.; Auster, U.; et al. The Comet Interceptor Mission. *Space Sci. Rev.* **2024**, *220*, 9. [CrossRef]

Disclaimer/Publisher's Note: The statements, opinions and data contained in all publications are solely those of the individual author(s) and contributor(s) and not of MDPI and/or the editor(s). MDPI and/or the editor(s) disclaim responsibility for any injury to people or property resulting from any ideas, methods, instructions or products referred to in the content.